JTTEE5 15:604-609
DOI: 10.1361/105996306X147289
1059-9630/$19.00 © ASM International

Peer Reviewed

Development of Porous Anode Layers for the Solid Oxide Fuel Cell by Plasma Spraying

H. Weckmann, A. Syed, Z. Ilhan, and J. Arnold

(Submitted February 27, 2006; in revised form April 28, 2006)

This article focuses on the development of the anode layer for solid oxide fuel cells by plasma spraying. The composite (cermet) anode, developed by thermal spraying, consisted of nickel and yttria-stabilized zirconia (YSZ). The effect of different plasma-spraying technologies on the microstructure characteristics and the electrochemical behavior of the anode layer were investigated. Coatings were fabricated by spraying nickel-coated graphite or nickel oxide with YSZ using a Triplex II plasma torch under atmospheric conditions as well as a standard F4 torch under atmospheric or soft-vacuum conditions. The investigations were directed to have an open microporous structure, higher electrical conductivity, and catalytic activity of anode deposits. Porosity was investigated by measuring the gas permeability. Scanning electron microscopy and x-ray diffraction technologies were applied to examine the morphology, microstructure, and composition of the layers. Electrical conductivity measurements were carried out to determine the ohmic losses within the anode layer. The most promising layers were analyzed by measuring the electrochemical behavior to obtain information about catalytic activity and performance.

Keywords anode, electrical conductivity, electrochemical characterization, permeability, solid oxide fuel cell, Triplex II, vacuum plasma spraying

1. Introduction

Solid oxide fuel cells (SOFC) are promising energy-converting systems for the 21st century with a high total efficiency (Ref 1). In a fuel cell, the chemical energy, which is stored in fuel gases such as hydrogen, kerosene, or natural gas, is transformed directly into electrical energy and heat. One main focus of the current research activities is to ensure high-performance fuel cells fabricated by batch production techniques. There is a significant influence on the performance due to the fabrication technology with respect to the microstructure of the electrodes. High-temperature fuel cells are usually fabricated by sinter (Ref 1-3) or thermal spray techniques (Ref 1, 4-6). Among thermal spray techniques, atmospheric plasma spraying (APS) (Ref 5, 7), vacuum plasma spraying (VPS) (Ref 8, 9), and high-velocity oxyfuel spraying are the most widely used methods used for the production of SOFCs. One single cell generates an open circuit voltage (OCV) of about 1 V. Several conditions control the output power of a single cell, including, for example, its effective area, temperature, materials of components, production process, and structure. By the parallel or serial interconnection of several fuel cell units, an energy-generating system with an adapted output power can be realized.

The basic components in a fuel cell assembly are the fuel-supplied anode and the oxygen-delivered cathode, which are separated by an ionic conductive, gas-tight electrolyte. Among the three layers, the SOFC anode plays an important role. The anode has to provide the reaction sites for the electrochemical oxidation of the fuel gas such as hydrogen and carbon monoxide (H_2 and CO, respectively) to water (H_2O) and carbon dioxide (CO_2). Thus, the layer must have a high open porosity, represented by a low flow resistance, to guarantee a sufficient supply of fuel gases and the disposal of reaction products. To obtain a highly efficient fuel cell, the anode has to fulfill the following requirements: homogeneous pore and material distributions provide an increase in electrochemical active areas and reduce polarization resistance (Ref 10). The anode layer must show a high stability under reducing and oxidizing conditions and has to demonstrate high electronic and ionic conductivity as well as a high catalytic activity for the electrochemical reaction under operating conditions. The minimization of the electrode resistance (polarization and ohmic) represents one of the greatest challenges in obtaining high, stable power densities.

A cermet consisting of yttria-stabilized zirconia (YSZ) and nickel (Ni) is the most common material combination for the anode due to the good electrochemical catalytic property of Ni and the low thermal expansion coefficient of YSZ (Ref 11). For a further reduction of power losses by ohmic resistances, the anode has to show high electronic conductivity along with good ionic conductivity, which is possible by adding YSZ in the layer. Furthermore, triple phase boundaries (i.e., Ni, YSZ, and fuel gas interface) can be increased with a good proportion of YSZ to Ni. The ceramic phase in the layer improves the mechanical integrity of the highly porous layer. However, at least 30 vol% Ni is

This article was originally published in *Building on 100 Years of Success, Proceedings of the 2006 International Thermal Spray Conference* (Seattle, WA), May 15-18, 2006, B.R. Marple, M.M. Hyland, Y.-Ch. Lau, R.S. Lima, and J. Voyer, Ed., ASM International, Materials Park, OH, 2006.

H. Weckmann, BMW Group, Munich, Germany; and **A. Syed, Z. Ilhan,** and **J. Arnold,** German Aerospace Center (DLR), Stuttgart, Germany. Contact e-mail: hannes.weckmann@dlr.de.

necessary to obtain continuous electrically conducting nickel paths, based on theory of percolation (Ref 12). The use of nickel oxide (NiO) in combination with YSZ as a base material leads to an increasing porosity during SOFC operation when the NiO in the anode is reduced to pure Ni by the fuel gas. This transformation is accompanied by a decrease in volume and thus an increase in porosity (Ref 12, 13). Thermal spraying of the SOFC anodes also allows the use of pure Ni and NiO graphite as feedstock, where graphite serves as a pore builder. Most of the graphite burns out during spraying and remaining can be removed by postheating in a furnace. Under atmospheric conditions, oxidation of the pure Ni powders in the plasma jet and on the substrate can be observed (Ref 7).

The aim of this work is to compare the morphology and microstructure as well as the electrochemical behavior of anode layers for the SOFC sprayed with different plasma-spraying methods and different feedstock powders. Therefore, a variety of NiO/YSZ samples were sprayed under APS and VPS conditions, and were compared with APS-sprayed, Ni-coated graphite/YSZ anodes.

2. Experimental

2.1 Feedstock Material

The planar SOFC design fabricated by thermal-spraying techniques utilizes a porous metallic substrate on which the functional layers are deposited (Ref 9, 13). For this study, 650 μm thick porous (porosity about 40%) sintered ferritic steel substrates (25 wt.% Cr) were deposited. The button cells had a diameter of 47 mm and a thickness of 1 mm. These porous substrates were used for electrochemical testing and permeability measurements. For the electrical conductivity measurements of plasma-sprayed layers, grid-blasted alumina substrates were used due to their high specific resistance of about 1×10^{14} Ω/m (at room temperature) (Ref 14). Grid-blasted metal plates made of ferritic chromium steel (Crofer22APU, 48 × 48 × 0.5 mm) were coated for measuring the mass deposition efficiency and surface roughness.

The feedstock powders were 9.5 mol% YSZ (9.5YSZ) from H.C. Starck (Laufenburg, Germany) in combination with agglomerated NiO from Becon (Thun, Switzerland) for the experiments conducted under VPS conditions with the F4 torch, which represent the reference layers. For the experiments conducted under atmospheric conditions with the F4 torch, the same powders were used. For the experiments with the Triplex II torch (APS) (SulzerMetco, Winterthur, Switzerland), commercially available standard 8 mol% YSZ (8YSZ) in combination with nickel-coated graphite powders (75 wt.% Ni), both from SulzerMetco, were sprayed. Both YSZ powders are fused and crushed with similar grain size distributions, namely, in the range of –22 to +5 μm. The Ni-based powders were supplied in different size ranges. The NiO has a grain size distribution range of −54 to +15 μm, and the Ni-coated graphite powder has a grain size range of −69 to +21 μm. The specifications of the powders and the scanning electron microscope (SEM) micrographs of the NiO (Fig. 1a), the Ni-graphite (Fig. 1b), and the 9.5YSZ (Fig. 1c) are shown, respectively, in Fig. 1. The SulzerMetco 8YSZ is not displayed in Fig. 1, because its structure and its grain size distribution are similar to those of the H.C. Starck 9.5YSZ powder.

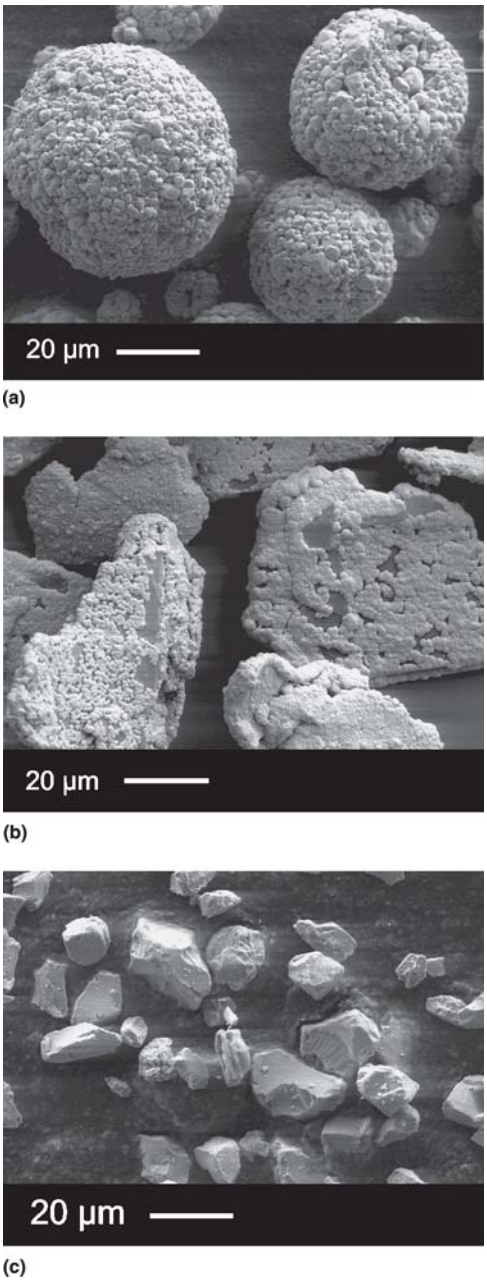

Fig. 1 Powder characteristics: (a) NiO, Becon/CH, −54 to +15 μm; (b) Ni-coated graphite, SulzerMetco/CH, −69 to +21 μm (sieved), composition 75 wt.% Ni/25 wt.% graphite; and (c) ZrO_2 9.5 mol% Y_2O_3 H.C. Starck/D, −22 to +5 μm (not displayed ZrO_2 8 mol% Y_2O_3, SulzerMetco/CH, −21 to +7 μm).

2.2 Spray Parameters

Anode coatings were made by plasma spraying under vacuum (reference) and under atmospheric conditions with an F4 torch at the German Aerospace Center (DLR; Stuttgart, Germany). The spraying process was controlled by a VIP 6000 sys-

Table 1 Plasma spraying parameters used to fabricate anode coatings under APS and VPS conditions

Parameter	VPS (F4)	APS	
		F4	Triplex II
Ambient pressure, mbar	200	Atmospheric	Atmospheric
Arc current, A	550	600	350
Stand-off distance, mm	240	100	110
Plasma gas flow, slpm	38Ar/4H_2/10He	35Ar/3H_2/15He	45Ar
Relative velocity plasma-substrate, mm/s	400	400	1050
Injection	Ø 3 mm, 15°	Ø 3mm, 15°	Ø 1,8 mm, 0°
Nozzle	Mach3/7 mm	F4V	9 mm standard

tem (GTV, Luckenbach, Germany). For the experiments under VPS conditions, a Mach 3 converging-diverging nozzle and for experiments under atmospheric conditions, F4 V nozzle were used. The YSZ and the NiO were injected separately into the F4 torch by two twin powder feeders (GTV). The challenge was to inject and melt the different materials with different melting temperatures (T_m) (YSZ < 2700 °C; NiO 1984 °C) in the torch to achieve homogeneous material distribution within the deposited layer. The YSZ and NiO powders were fed into the plasma from two 3 mm diameter injectors positioned radially and pointing 15° downstream into the plasma jet, respectively. The layers under vacuum conditions were sprayed with a mean (± standard deviation) NiO content of 48 ± 2 vol.% (28 ± 2 vol.% Ni after reduction). The base powder for the samples sprayed under APS conditions had a content of 50 vol.% NiO (respectively 30 vol.% Ni after reduction) and 50 vol.% YSZ.

The experiments with the Triplex II torch were carried out at SulzerMetco, CH, under APS conditions. The Triplex II torch was equipped with a 9 mm standard nozzle. Prior to spraying, the YSZ powder was mixed with the Ni-coated graphite powder (T_m for Ni 1453 °C) in a Retsch mill for 15 min. The ratio of the mixture was 50 wt.% YSZ and 50 wt.% Ni-coated graphite. Three independent twin powder feeders transported the powder mixture into the torch where the powder was fed into the plasma from three 1.8 mm diameter injectors positioned radially and perpendicular to the torch axis. There was no active substrate-cooling device installed in all experiments to prevent microcracks in the ceramic phase. Various sets of parameters were tested under APS and VPS conditions. In Table 1, the parameters for the reference coating under vacuum conditions and the most promising parameters for the anode layers sprayed under atmospheric conditions are listed. After spraying, the Ni-coated, graphite-based anode deposited by the Triplex II gun revealed only traces of remaining carbon, as examined by SEM. Therefore, no posttreatment was conducted.

To characterize the deposited anode layers electrochemically, an electrolyte layer was sprayed additionally onto the anodes, and finally an $(La_{0,8}Sr_{0,2})_{0,98}MnO_3$ (LSM) cathode was screen printed on the electrolyte. The electrolyte layer was 45 μm thick, VPS-sprayed 9.5YSZ (H.C. Starck) . The spray parameters for the electrolyte are listed elsewhere (Ref 15).

2.3 Characterization of Coatings

The morphology and the microstructure of the coatings were examined using a LEO 982 Gemini SEM (Zeiss, Oberkochen, Germany) with secondary and backscattered electron detectors. Surface roughness measurements (R_a) were realized with a mobile Hommel Tester T500 (Hommelwerke, Villingen-Schwenningen, Germany). Lateral (in-plane) electrical conductivity was measured by a 4-point measurement method at DLR. Permeability was measured with the pressure drop method in which a constant transversal gas flow causes a flow resistance (pressure drop) through the anode layer. Synthetic air (80 mol% N_2, 20 mol% O_2) was used for these measurements. The effect of the porous substrate on the permeability coefficient α can be neglected because any resistance to airflow due to the substrate is sufficiently low and is within the accuracy of the measuring device. The following equation was used to calculate the permeability coefficient α (Ref 16, 17).

$$\alpha = \frac{Q \cdot \eta \cdot d}{A \cdot \Delta p} \quad [\mathrm{m}^2]$$

where Q is the gas flow rate through the porous layer (in cubic meters per second), η is the viscosity of synthetic air (in newtons per square meter), d is the thickness of the layer (in meters), A is the area of the layer (in square meters), and Δp is the pressure drop over the layer (in newtons per square meter).

To have information about the permeability under operating conditions, some of the NiO anode layers were reduced by heating in a furnace over 5 h to 900 °C under a reducing atmosphere (purge gas with 95% Ar and 5% H_2). The furnace temperature was then held at 900 °C for 1.5 h followed by cooling down to room temperature in 5 h. During the reduction heat treatment, the samples were loaded with 30 g/cm^2 of pressure by alumina cylinders to keep the sample flat.

3. Results and Discussion

The surface roughness of the anode layer is an important quality for the subsequent electrolyte layer. It is more difficult to deposit a 40 μm thin gas-tight electrolyte on anodes having high roughness. On the other hand, a smooth surface can prohibit sufficient adhesion of the electrolyte coating. An optimum roughness value is so far unknown. Table 2 shows the surface roughness of different anode samples. The surface topography of the samples produced under atmospheric conditions is rougher than the surface of the reference coating, which was sprayed under soft-vacuum conditions. One reason for this might be the higher particle velocity resulting from vacuum spraying. No significant difference in the roughness (R_a) between the coating with NiO/YSZ cermet (F4 gun) and the cermet made of Ni-graphite/YSZ (Triplex II gun) was measured.

Permeability of the plasma-sprayed anode layer is an essen-

Table 2 Surface roughness of anodes produced by different spraying processes

		APS	
Variables	**VPS (F4)**	**F4**	**Triplex II**
Material	NiO/9.5YSZ	NiO/8YSZ	Ni-graphite/8YSZ
Condition	As sprayed	As sprayed	As sprayed
R_a, μm	3.7	5.0	5.4

tial quality for the operation of the anode in an SOFC. Flow resistance determines the power losses, especially at high power outputs and high gas exchange rates. The permeability coefficients α for the investigated samples are shown in Fig. 2. For the coatings containing NiO, it can be observed that the permeability coefficient after reduction is higher and thus flow resistance decreases significantly after reduction. This is due to the transformation of the NiO to Ni accompanied by the increase in porosity within the layer. Because in former investigations no change in permeability between the as-sprayed and the reduced Ni-graphite/YSZ layers was measured, only one permeability coefficient is shown for this case.

In Fig. 3, the temperature-dependent performance of the specific electronic conductivity for all three anode layers is shown. The reference anode shows the lowest electrical conductivity of 1.6×10^2 S/cm at 775 °C. One reason for this might be the lamellar structure with a lack of electronic conducting paths and the low Ni content in the base powder. With 4.4×10^2 S/cm at 775 °C, the specific conductivity of the sample sprayed with the 30 vol.% Ni under APS conditions is a little bit higher due to the higher content of Ni in the base powder. The sample with the highest nickel content (APS, Triplex II gun) has the highest conductivity (1.0×10^3 S/cm at 775 °C).

As shown in Fig. 3, the sharp bends in all three curves at 360 °C correspond to the Curie point of Ni, where a change from ferromagnetic behavior to paramagnetic behavior takes place. With this bend, it can be suggested that the measured curves represent metallic conductivity. In Fig. 4, the time-dependent variation of the specific electronic conductivity for the three anode layers is given. The APS NiO and the Ni-graphite cermet coatings show a slight improvement in conductivity values over 38 h. A similar behavior can often be observed in fuel cells within the first 100 h. This might happen due to the development of electronic conducting paths in the layer. Only the reference VPS-sprayed NiO/YSZ cermet shows a slight decrease of conductivity during the first 10 h and stabilizes later up to 38 h.

The quality of an anode layer depends strongly on its microstructure. A high open porosity in combination with a good material distribution of nickel and YSZ is demanded.

In Fig. 5, optical micrographs of the polished cross sections of the coatings are displayed. Both NiO coatings produced with the F4 torch have relatively dense and typical lamellar structures. Almost no pure metallic phase can be detected in the as-sprayed layers. Only in the reference coating there are some bright white spots, which represent pure Ni. The Ni-graphite/YSZ layer is much rougher and more porous, consisting of pure Ni and a small amount of carbon. It is not clear whether this remaining carbon may have an adverse effect on anode performance during cell operation. One reason for the rough structure of the Ni-graphite anode might be the bursting of the Ni-covered graphite particles when impinging on the substrate.

Two fuel cells (one cell with a reference anode and one cell with a nickel-graphite anode) were characterized electrochemically. The electrochemical test setup and procedures for measurements have been described elsewhere (Ref 18). The most

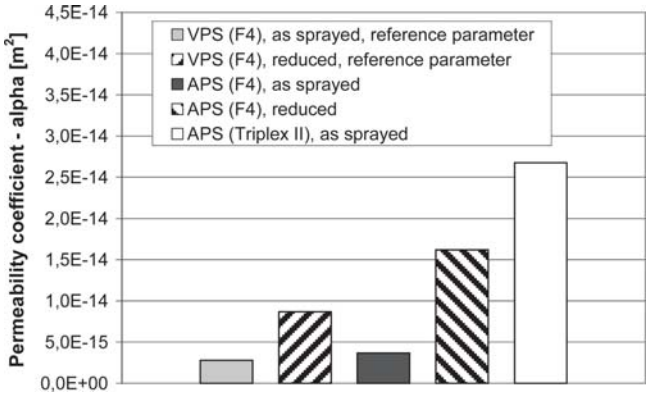

Fig. 2 Permeability as a function of the spraying process

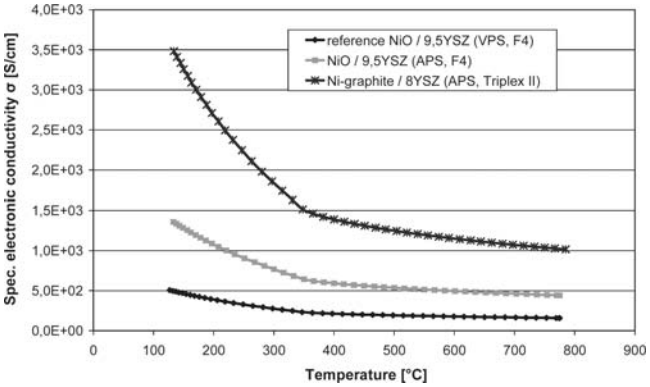

Fig. 3 Specific electrical conductivity of the plasma-sprayed anode layers as a function of temperature

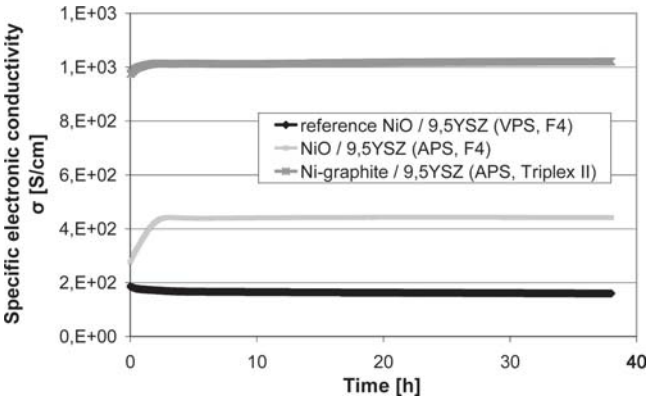

Fig. 4 Specific electrical conductivity of the plasma-sprayed anode layers as a function of time at 775 °C

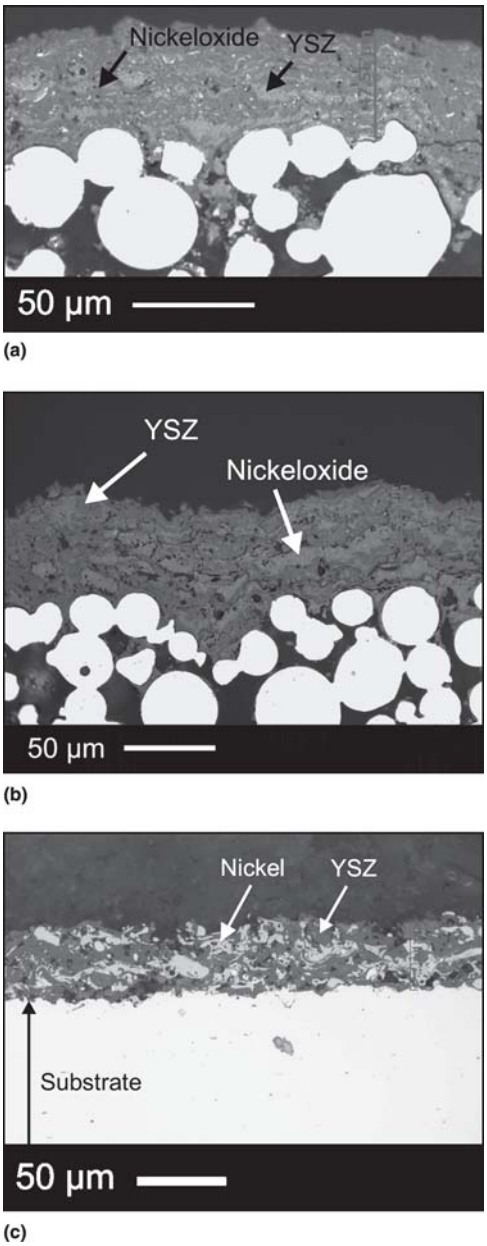

Fig. 5 Optical micrograph of polished cross sections of (a) reference coating sprayed under soft-vacuum conditions ($p_{chamber}$ = 200 mbar) and optimized anode coatings sprayed under atmospheric conditions with (b) a F4 torch and (c) a Triplex II torch. All pictures show coatings in the as-sprayed state.

important electrochemical results of the first cell, consisting of a standard anode layer (VPS, NiO/YSZ) are presented in Fig. 6. The OCV gives information about the density of the electrolyte. A moderate OCV of 1.028 V after activation may be due to the dense anode prohibiting fuel gas to reach the electrolyte. The OCV stabilizes to a higher value of about 1.042 V after 86 h of operation due to the increased permeability of the reduced anode (as shown in Fig. 2). Power density increases during operation from 70 to 200 mW/cm^2 as a result of the activation processes in the electrodes. The formation of electronic conductive paths in the Ni/YSZ cermet is one reason for such an activation process.

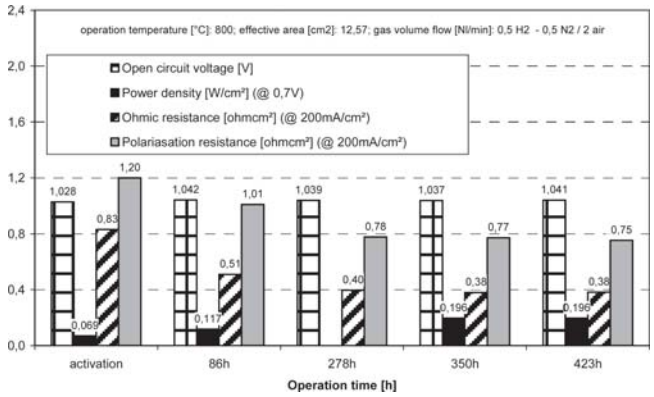

Fig. 6 Electrochemical results for the cell equipped with the reference anode (VPS, NiO/YSZ) showing OCV, power density, ohmic resistance, and polarization resistance as a function of operation time

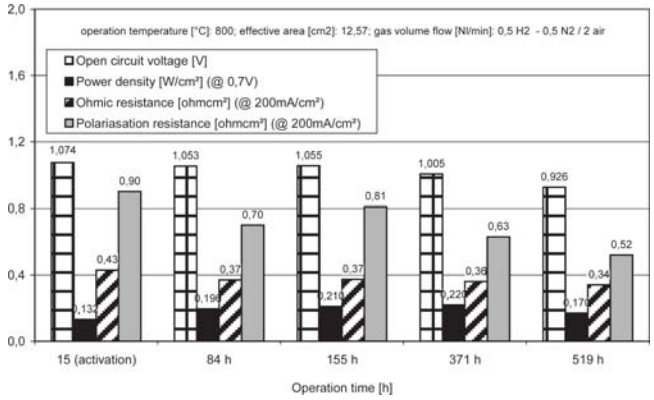

Fig. 7 Electrochemical results for the cell equipped with the Ni-graphite anode (Triplex II torch) showing OCV, power density, ohmic resistance, and polarization resistance as a function of operation time

The decline of the polarization resistance from 1.20 to 0.75 Ωcm^2 results from the activation process, mainly in the cathode, which appears during start up when the loose particles of the cathode contact paste sinter together. The decrease in ohmic resistance is determined by the improvement in electrode contact, especially in the cathode and the formation of electric conductive paths. After 278 h, the total resistance remains almost constant. Performance of the cell consisting of the Ni-graphite/YSZ anode is better in terms of higher OCV and lower total resistance (Fig. 7). The lower total resistance can be correlated with the results from conductivity measurements (compared to Fig. 3). The measured ohmic resistance of the Ni-graphite cell after activation is similar to that of the NiO cell. One conclusion from this observation is that the assembly of the cells was reproducible and contact resistances are almost equal. Ohmic resistance in the Ni graphite cell remains constant for the entire operation time. The polarization resistance decreases from 0.90 to 0.52 Ωcm^2. Due to the same assembly of both cells, the difference in the polarization resistance results from the different anodes, and the Ni-graphite cell therefore has a better performance. The decrease of OCV might be due to leakage in the cell sealing or microcracks in the electrolyte. After 400 h of operation, an op-

erating-gas malfunction caused the oxidation of the anode, which was accompanied by an increase in anode volume and finally led to microcracks in the electrolyte layer. A drastic decrease in OCV to 0.926 V was the result.

4. Summary

In the current study, the influence of different plasma-spraying technologies on the permeability, electrical conductivity, and electrochemical behavior of Ni/YSZ coatings for SOFC applications was investigated. Cermet layers were produced by spraying Ni-coated graphite and YSZ using a Triplex II plasma torch under atmospheric conditions, and NiO in combination with YSZ using an F4 torch under soft vacuum as well as atmospheric conditions. The surface roughness as an important property for the adhesion and the build up of the subsequent electrolyte layer and for the contact of the fuel cell with the interconnector was higher in both atmospheric sprayed layers. Electrical conductivity measurements concluded that the major difference in conductivity arises from the Ni content in the deposit. The permeability of the Ni-graphite layer sprayed with the Triplex II torch was the highest due to its very porous structure. The atmospheric sprayed NiO/YSZ coating had a better permeability than the reference layer sprayed under soft vacuum conditions. The microstructure of the reference layer and the developed NiO/YSZ coating did not differ drastically. The Ni-graphite/YSZ coating however had a very porous structure varying from the typical lamellar build up of thermal-sprayed coatings. The fuel cell equipped with the Ni-graphite/YSZ (Triplex II torch) anode showed better electrochemical performance than the cell sprayed with the reference parameters under soft vacuum conditions (NiO/YSZ) due to higher OCV and lower resistance. However, the Ni-graphite cell showed stronger degradation behavior in OCV over the operation time (partially due to an operating-gas malfunction after 300 h).

References

1. N.Q. Minh and T. Takahashi, *Science and Technology of Ceramic Fuel Cells,* Elsevier, 1995
2. S.D. Kim, S.H. Hyun, M. Jooho, K. Jong-Hee, R. Hyon Song, D. Simwonis, H. Thule, F.J. Dias, A. Naoumidis, and D. Stöver, Fabrication and Characterization of Anode-Supported Electrolyte Thin Fils for Intermediate Temperature Solid Oxide Fuel Cells, *J. Power Sources,* 2005, **139,** p 67-72
3. D. Simwonis, H. Thule, F.J. Dias, A. Naoumidis, and D. Stöver, Properties of Ni/YSZ Porous Cermets for SOFC Anode Substrates Prepared by Tape Casting and Coat-Mix Process, *J. Mater. Proc. Technol.,* 1999, **92-93,** p 107-111
4. K. Okumura, Y. Aihara, S. Ito, and S. Kawasaki, Development of Thermal Spraying-Sintering Technology for Solid Oxide Fuel Cells, *J. Thermal Spray Technol.,* 2000, **9**(3), p 354-359
5. X.Q. Ma and S. Hui, Intermediate Temperature SOFC Based on Fully Integrated Plasma Sprayed Components, *Thermal Spray 2003: Advancing the Science and Applying the Technology,* B.R. Marple and C. Moreau, Ed., May 5-8, 2003 (Orlando, FL), ASM International, 2003 p 163-168
6. H.C. Chen, J. Heberlein, and R. Henne, Integrated Fabrication Process for Solid Oxide Fuel Cells in a Triple Torch Plasma Reactor, *J. Thermal Spray Technol.,* 2000, **9**(3), p 348-353
7. H. Weckmann, O. Finkenwirth, R. Henne, and A. Refke, Microstructure of Ni-Graphite/YSZ Composite Coatings on Porous Metallic Substrates Obtained by Atmospheric Plasma Spraying (APS), *Thermal Spray Connects: Explore Its Surfacing Potential,* E. Lugscheider, Ed., DVS, Düsseldorf, Germany, 2005
8. A. Refke, G. Barbezat, D. Hawley, and R.K. Schmid, Low Pressure Plasma Spraying (LPPS) as a Tool for the Deposition of Functional SOFC Components, *Thermal Spray Solutions, Advances in Technology and Application,* DVS, Düsseldorf, Germany, 2004
9. G. Schiller, R. Henne, M. Lang, and M. Müller, DC and RF Plasma for Fabrication of Solid Oxide Fuel Cells, *Thermal Spray Solutions, Advances in Technology and Application,* DVS, Düsseldorf, Germany, 2004
10. A. Weber, Development of Cathode Structures for the Solid Oxide Fuel Cell SOFC, Ph.D. dissertation, University of Karlsruhe, 2002, in German
11. J.-H. Lee, H. Moon, H.-W. Lee, J. Kim, J.-D. Kim, and K.-H. Yoon, Quantitative Analysis of Microstructure and Its Related Electrical Property of SOFC Anode, Ni-YSZ Cermets, *Solid State Ionics,* 2002, **148,** p 15-26
12. D.W. Dees, T.D. Claar, T.E. Easler, D.C. Fee, and F.C. Mrazek, Conductivity of Porous Nickel / Zirconia Cermets, *J. Electrochem. Soc.,* 1987, **134**(9), p 2141-2146
13. M. Lang, Development and Characterization of Vacuum Plasma Sprayed ZrO2/Ni-Anodes for Solid Oxide Fuel Cells, Ph.D. thesis, University of Stuttgart, 1999 (in German)
14. W. Gao and N.M. Sammes, *An Introduction to Electronic and Ionic Materials,* World Scientific Publisher, 1999
15. A.A. Syed, Z. Ilhan, H. Weckmann, J. Arnold, and G. Schiller, Improving Plasma Sprayed YSZ Coatings for SOFC Electrolytes, *Building on 100 Years of Success: Proceedings of the 2006 International Thermal Spray Conference,* B.R. Marple, M.M. Hyland, U.-Ch. Lau, R.S. Lima, and J. Voyer, Ed., May 15-18, 2006 (Seattle, WA), ASM International, 2006
16. "Permeable Sinter Metals: Evaluation of the Specific Permeability," DIN ISO 4022, Berlin, 1990, in German
17. Mould List: High Porous Sintered Bronze, *GKN Sinter Metals,* Radevormwald, Germany, 2005
18. T. Franco, M. Lang, G. Schiller, P. Szabo, W. Glatz, and G. Kunschert, Powder Metallurgical High Performance Materials for Substrates-Supported IT-SOFCs, *6th European SOFC Forum,* M. Mogensen, Ed., European Fuel Cell Forum, June 28-July 2, 2004 (Lucerne, Switzerland), 2004, p 209-217